# *STCLocker*: Deadlock Avoidance Testing for Autonomous Driving Systems

Mingfei Cheng
Singapore Management University
Singapore

Renzhi Wang
University of Alberta
Canada

Xiaofei Xie
Singapore Management University
Singapore

Yuan Zhou
Zhejiang Sci-Tech University
China

Lei Ma
The University of Tokyo
Japan
University of Alberta
Canada

arXiv:2506.23995v1 [cs.SE] 30 Jun 2025

## Abstract

Autonomous Driving System (ADS) testing is essential to ensure the safety and reliability of autonomous vehicles (AVs) before deployment. However, existing techniques primarily focus on evaluating ADS functionalities in single-AV settings. As ADSs are increasingly deployed in multi-AV traffic, it becomes crucial to assess their cooperative performance, particularly regarding deadlocks, a fundamental coordination failure in which multiple AVs enter a circular waiting state indefinitely, resulting in motion planning failures. Despite its importance, the cooperative capability of ADSs to prevent deadlocks remains insufficiently underexplored. To address this gap, we propose the first dedicated Spatio-Temporal Conflict-Guided Deadlock Avoidance Testing technique, *STCLocker*, for generating DeadLock Scenarios (DLSs), where a group of AVs controlled by the ADS under test are in a circular wait state. *STCLocker* consists of three key components: *Deadlock Oracle*, *Conflict Feedback*, and *Conflict-aware Scenario Generation. Deadlock Oracle* provides a reliable black-box mechanism for detecting deadlock cycles among multiple AVs within a given scenario. *Conflict Feedback* and *Conflict-aware Scenario Generation* collaborate to actively guide AVs into simultaneous competition over spatial conflict resources (i.e., shared passing regions) and temporal competitive behaviors (i.e., reaching the conflict region at the same time), thereby increasing the effectiveness of generating conflict-prone deadlocks. We evaluate *STCLocker* on two types of ADSs: *Roach*, an end-to-end ADS, and *OpenCDA*, a module-based ADS supporting cooperative communication. Experimental results show that, on average, *STCLocker* generates 3.39× more DLS than the best-performing baseline. By shifting the focus from single-AV evaluation to multi-AV cooperation, our approach offers a novel and realistic perspective for ADS testing, pushing the boundaries of reliability assessment in autonomous driving systems.

## 1 Introduction

Autonomous Driving Systems (ADSs) have rapidly advanced in recent years, offering the potential to significantly improve transportation efficiency and urban mobility. As the central control unit of autonomous vehicles (AVs), an ADS is responsible for enabling the vehicle to operate safely without human intervention. Modern ADSs integrate artificial intelligence algorithms with symbolic reasoning to perceive and understand their environment using data from a variety of sensors, including cameras, LiDAR, radar, and GPS. Based on this perception, the ADS performs key functions such as decision-making, motion planning, and control to ensure safe and efficient driving. Despite the substantial progress in ADS development over the past decades, ensuring that these systems can consistently meet performance requirements across diverse and unpredictable driving scenarios remains a significant challenge, due to inherent vulnerabilities and limitations [18]. As a result, comprehensive testing of ADSs across a wide range of conditions is essential before they can be safely deployed in the real world [37].

Simulation-based ADS testing has made significant progress in uncovering weaknesses in ADSs. Existing efforts primarily fall into two categories: (1) reconstructing scenarios based on real-world accidents [21, 53, 63]; and (2) designing algorithms to generate scenarios that target specific testing objectives, such as inducing collisions [8, 24, 25, 29, 32, 35, 38, 74], violating traffic rules [36, 52, 72], or evaluating non-safety-critical properties such as decision optimality [7]. However, most of existing works only focus on single-vehicle settings, where the ADS is tested within a single autonomous vehicle and other NPC vehicles. Such settings fail to capture the complexity of real-world deployments, where multiple AVs operate concurrently and interact dynamically. For instance, commercial platforms like Waymo One [66] and Apollo Go [4] have deployed thousands of autonomous vehicles in urban environments. These large-scale deployments have occasionally worsened traffic conditions, leading to incidents such as collisions and congestion [5, 12], highlighting the need for more comprehensive testing in multi-AV scenarios.

This paper aims at the testing challenges that arise from the deployment of multiple autonomous vehicles, with a particular focus on *deadlock* scenarios in their cooperative behavior. Effective cooperation among AVs is essential for ensuring safe and efficient interactions in dense traffic environments. Deadlocks can occur when two or more AVs, each controlled by the ADS, attempt to pass through a common region but end up waiting for one another to proceed, ultimately resulting in a circular wait. Fig. 1 illustrates an example of a deadlock at an intersection. As shown in Fig. 1(a), both AVs are proceeding through the intersection: AV 1 is going straight, while AV 2 is making a left turn. However, as they approach the shared conflict point, AV 1 detects that AV 2 intends to turn left and decides to stop to let AV 2 pass first. At the same time, AV 2 also stops, waiting for AV 1 to proceed first. This circular wait results in a deadlock, as illustrated in Fig. 1(b). Such deadlocks can completely

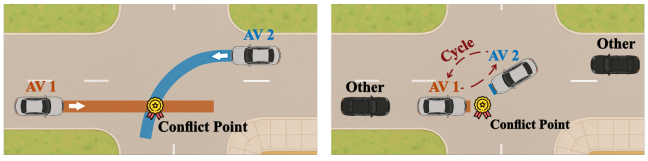



**Figure 1: Illustration of a deadlock scenario.**

halt traffic flow, block other vehicles and entire road segments, and lead to broader negative impacts on transportation efficiency and societal well-being. Therefore, it is crucial to develop systematic testing techniques to evaluate the deadlock-handling capabilities of ADSs in multi-AV scenarios.

To the best of our knowledge, there is limited research on evaluating the ADS cooperative abilities among multiple AVs, specifically, the capability to avoid deadlocks [51]. Although some existing ADS testing techniques, such as DoppelTest [29], started to test scenarios with multiple autonomous vehicles, their objective remains focused on identifying individual weaknesses of the ADS under test in single-AV settings, such as determining its responsibility in violations, rather than evaluating its global cooperation in multi-AV scenarios.

To fill this gap, we present the first study on evaluating the cooperative abilities of ADSs in multi-AV settings, with a particular focus on assessing their capability to avoid deadlocks. However, AV deadlock detection poses two major technical challenges. ❶ First, deadlocks are difficult to identify based solely on temporary stationary behavior without access to high-level semantic intentions. ADSs, particularly those based on deep learning models, do not expose internal semantic states, making it challenging to infer the underlying inter-vehicle dependencies necessary for accurate deadlock detection. ❷ Second, deadlocks are sparsely distributed in the scenario space and typically emerge only under specific interactions, road geometries, and traffic configurations. For example, given $N$ vehicles and $M$ possible motion choices per vehicle, the joint configuration space scales exponentially as $N^M$, rendering exhaustive exploration infeasible. The complexity further increases when factoring in road topology and vehicle positions, leading to an even larger and more complex search space. Therefore, effectively identifying traffic and interaction patterns that are prone to deadlock remains a challenge.

To address these challenges, we propose *STCLocker*, a novel *Spatio-Temporal Conflict-Guided Deadlock Avoidance Testing* method, designed to effectively identify and generate deadlock scenarios (DLSs) in multi-AV environments. *STCLocker* consists of three main components: *Deadlock Oracle*, *Conflict Feedback*, and *Conflict-aware Scenario Generation*. To tackle the first challenge ❶, *Deadlock Oracle* provides a reliable mechanism for identifying deadlock cycles among multiple AVs by predicting and abstracting low-level observable behaviors into semantic edges in a wait-for graph. This abstraction facilitates the detection of cyclic dependencies that signify deadlocks. To address the second challenge ❷, we design *Conflict Feedback* and *Conflict-aware Scenario Generation* to collaboratively guide multiple AVs into deadlock states. Specifically, *Conflict Feedback* provides guidance by jointly analyzing spatial conflict regions among trajectories and the temporal behaviors of AVs near the identified regions. Guided by this feedback, *Conflict-aware Scenario Generation* adjusts both the spatial routes and temporal attributes (i.e., trigger times) of the scenarios to generate more conflict-prone interactions among AVs, thereby increasing the likelihood of inducing deadlocks.

We evaluate *STCLocker* on the high-fidelity simulator CARLA [11] with two ADSs: *Roach* [73], an end-to-end model-based ADS, and *OpenCDA* [68], a modular ADS that supports cooperative communication. We compare *STCLocker* against two baselines: *Random*, which randomly generates multi-AV scenarios, and *DoppelTest* [29], which evaluates ADSs in multi-AV settings with a focus on multiple safety-critical properties. Experimental results demonstrate that *STCLocker* is both effective and efficient in generating DLSs, revealing the limited cooperative capabilities of current ADSs in avoiding deadlocks. For example, *STCLocker* successfully generates a total of 188.2 DLSs, while the best-performing baseline detects only 58.8 DLSs. Further ablation studies confirm the contribution of each component in *STCLocker*.

In summary, this paper makes the following contributions:

(1) We present the first study that systematically evaluates the cooperative capabilities of ADSs in multi-AV settings, with a particular focus on their ability to avoid deadlocks, which is a critical yet underexplored non-safety-critical property.
(2) We propose a novel search-based method, *STCLocker*, which effectively identifies and generates deadlock scenarios (DLSs) through spatial and temporal conflict guidance.
(3) We conduct extensive experiments on two distinct types of ADSs to demonstrate the effectiveness of *STCLocker* and to reveal significant limitations in their cooperative behavior under potential deadlock conditions.

## 2 Background

### 2.1 Autonomous Driving Systems

Autonomous Driving Systems (ADSs) serve as the decision-making core of autonomous vehicles, generating driving actions based on perceived environmental context. Existing ADSs can generally be categorized into two main paradigms: module-based and end-to-end (E2E). Module-based ADSs, such as Baidu Apollo [3], Autoware [31], and Pylot [20], are composed of distinct components, typically including perception, prediction, planning, and control. Each module is responsible for a specific subtask that collectively ensures safe and effective vehicle operation. The perception module processes raw sensor data (e.g., camera images and LiDAR point clouds) to detect and interpret environmental elements such as nearby vehicles, primarily using deep learning (DL) models. The prediction module estimates the future motion of surrounding objects based on the perception outputs. Given the results of the perception and prediction modules, the planning module generates a safe and feasible trajectory for the vehicle to follow. Finally, the control module translates this trajectory into low-level control commands (e.g., steering, throttle, and braking) to execute the planned motion. With the rapid advancement of deep learning, end-to-end (E2E) ADSs seek to replace traditional module-based architectures with unified deep learning models. For example, UniAD [27] and OpenPilot [9] employ models that directly map sensor inputs to

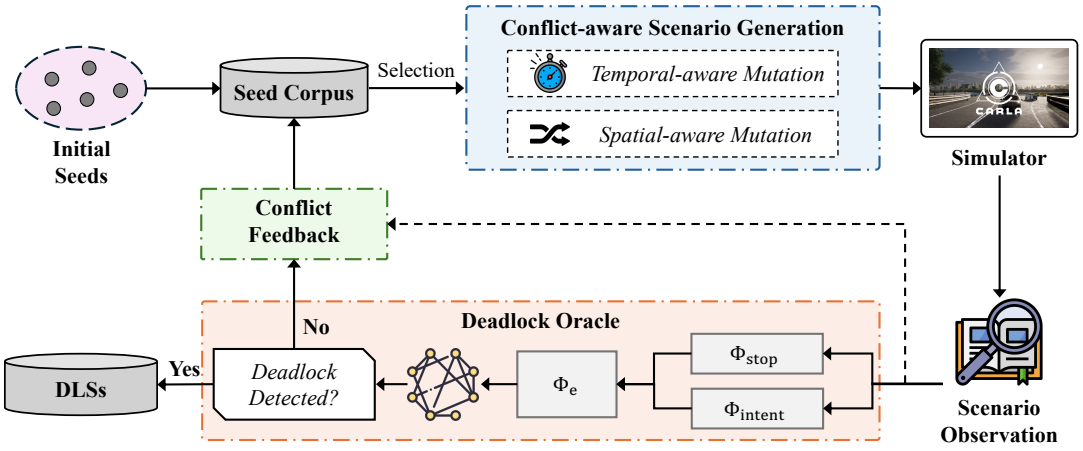



**Figure 2: Overview of *STCLocker*.**

driving commands, bypassing the need for explicit modular decomposition. Other approaches adopt a hybrid paradigm by replacing only specific components within conventional ADSs. Methods such as PlanT [48] and Interfuser [50] map sensor data to planned trajectories, while still relying on conventional rule-based controllers (e.g., PID) for low-level vehicle control. Roach [73], for instance, replaces the decision-making module, taking outputs from the perception system and generating control commands directly.

## 2.2 Scenario

Testing Autonomous Driving Systems (ADSs) requires a diverse collection of scenarios as testing inputs. Each scenario is typically defined by a set of parameters that specify the environment (e.g., road layout, weather conditions) and traffic participants, including Non-Player Character (NPC) vehicles, pedestrians, and static obstacles. Complex scenarios are often constructed by combining relevant attributes derived from the Operational Design Domains (ODDs)[60]. However, exhaustively covering all attribute combinations is infeasible due to the vastness of the attribute space. Therefore, following prior work[8, 24, 29, 32, 35, 38, 62], we select representative subsets of attributes for the purpose of deadlock testing. Formally, a *scenario* can be represented as a tuple $S = \{\mathcal{A}, \mathcal{P}\}$, where $\mathcal{A} = \{\text{AV}_1, \ldots, \text{AV}_{|\mathcal{A}|}\}$ is a finite set of autonomous vehicles (AVs) controlled by the ADS under test, $\mathcal{P} = \{P_1, \ldots, P_{|\mathcal{P}|}\}$ is a finite set of traffic participants, such as dynamic NPC vehicles. Specifically, each autonomous vehicle $\text{AV}_i$ is defined as a tuple $\text{AV}_i = \{p_i^{\text{start}}, p_i^{\text{dest}}, t_i^{\text{trigger}}\}$, where $p_i^{\text{start}}$ and $p_i^{\text{dest}}$ denote the starting position and destination, respectively, and $t_i^{\text{trigger}}$ indicates the trigger time at which the vehicle begins to move. Each participant $P_i \in \mathcal{P}$ is represented as a sequence of waypoints $P_i = \{w_i^1, \ldots, w_i^{N_i}\}$, where $N_i$ denotes the number of waypoints. Each waypoint $w = \{p, \theta, v\}$ encodes the position $p$, heading angle $\theta$, and expected speed $v$. *Scenario observation* refers to a sequence of scenes that capture the execution of a scenario within a simulation. Formally, given a scenario $S$, its observation is denoted as $O(S) = \{\mathbf{o}_0, \ldots, \mathbf{o}_T\}$, where $T$ is the length of the observation and $\mathbf{o}_t$ represents the scene at timestamp $t$. In detail, at timestamp $t$, the scene observation is denoted as $\mathbf{o}_t = \{y_t^j \mid j \in \{\mathcal{A} \cup \mathcal{P}\}\}$, where $y_t^j$ represents the observation of the $j$-th participant. Each observation is defined as $y_t^j = \{p_t^j, \theta_t^j, v_t^j, a_t^j\}$, which includes the center position $p_t^j$, heading angle $\theta_t^j$, velocity $v_t^j$, and acceleration $a_t^j$ at timestamp $t$. By default, we use $O(\mathcal{A})$ to denote the set of AV observations in scenario $S$, where each $\mathbf{o}_t \in O(\mathcal{A})$ is defined as $\mathbf{o}_t = \{y_t^j \mid j \in \mathcal{A}\}$.

# 3 Problem Definition

This paper aims to evaluate deadlock situations that occur during the deployment of an ADS across multiple autonomous vehicles (AVs) operating in traffic. Following the deadlock definitions in prior work [46, 47], we define the deadlock scenario (DLS) as follows:

*Definition 3.1 (Wait-for Graph).* Given a scenario $S$ and its observation $O(S)$, the wait-for graph with respect to $\mathbf{o}_t$ is defined as $G_t = (\mathcal{V}, \mathcal{E}_t)$. Here, $\mathcal{V} = \mathcal{A}$ is the set of vertices, each representing an AV, and $\mathcal{E}_t \subseteq \mathcal{V} \times \mathcal{V}$ is the set of directed edges at time $t$. A directed edge $e_t^{i \to j} \in \mathcal{E}_t$ indicates that $\text{AV}_i$ is waiting for $\text{AV}_j$ to move at timestamp $t$.

*Definition 3.2 (Deadlock Scenario).* A scenario $S$ is called a deadlock scenario, if there exists a scene $\mathbf{o}_t \in O(S)$ such that its coorresponding wait-for graph $G_t = (\mathcal{V}, \mathcal{E}_t)$ satisfies $\{e_t^{i_1 \to i_2}, e_t^{i_2 \to i_3} \ldots, e_t^{i_k \to i_1}\} \subseteq \mathcal{E}_t$.

A deadlock occurs when a group of AVs enters a circular wait, with each vehicle blocked by another in the group. As a result, they occupy shared traffic resources without making progress, potentially causing severe congestion. As illustrated in Fig. 1, such deadlocks can significantly degrade traffic efficiency. The goal of deadlock testing is to generate scenarios that induce deadlock among AVs without violating safety constraints. Notably, deadlocks can occur in both communication-enabled and communication-free settings.

# 4 Methodology

## 4.1 Overview

Fig. 2 presents a high-level overview of *STCLocker*, which generates DeadLock Scenarios (DLSs) from initial seed scenarios. *STCLocker* consists of three core components: *Deadlock Oracle*, *Conflict Feedback*, and *Conflict-aware Scenario Generation*. Specifically, *Deadlock*

**Algorithm 1:** Workflow of *STCLocker*

```
   Input  : Initial seed corpus Q
   Output : Deadlock scenario set F
1  F ← {}
2  repeat
       // Select a seed from corpus
3      {S, φ_S} ← SeedSelection(Q)
       // Generate new scenarios
4      S' ← ScenarioGeneration(S, φ_S)
5      O(S') ← Simulator(S')
       // Analyze deadlock cycles
6      r ← DeadlockOracle(O(S'))
7      if r is Fail then
8          F ← F ∪ {S'} // Update failure sets
9      else
           // Update seed corpus
10         φ_S' ← ConflictFeedback(O(S'))
11         if φ_S' < φ_S then
12             Q ← Q ∪ {S'} // Update seed corpus
13 until given time budget expires;
14 return F
```

*Oracle* constructs a wait-for graph based on observed AV behaviors and analyzes it to detect the presence of deadlock cycles. *Conflict Feedback* guides the testing process by analyzing spatial trajectory patterns and temporal interactions among the group of AVs. Based on the computed feedback scores, *Conflict-aware Scenario Generation* adaptively selects and applies either spatial-aware mutation or temporal adjustment strategies to increase the likelihood of inducing deadlocks.

Algorithm 1 outlines the core workflow of *STCLocker*, which follows a classical search-based testing paradigm. It maintains a seed corpus that is progressively enriched with high-potential scenarios to facilitate the efficient discovery of DLSs. Specifically, given an initial seed corpus $\mathbf{Q}$, *STCLocker* begins by initializing an empty set $\mathbf{F}$ to store the detected DLSs (Line 1). The testing process then proceeds iteratively until the specified time budget is exhausted, after which the set $\mathbf{F}$ is returned (Line 13). In each iteration, *STCLocker* first selects a seed $S$, along with its associated feedback score $\phi_S$, from the seed corpus $\mathbf{Q}$ (Line 3). Then, *Conflict-aware Scenario Generation* generates a new scenario $S'$ by modifying spatial and temporal attributes of $S$ based on $\phi_S$, with the goal of increasing inter-vehicle competitiveness and the likelihood of inducing deadlocks (Line 4). The scenario $S'$ is then executed in the simulator to obtain its observation $O(S')$ (Line 5). Based on this observation, *Deadlock Oracle* constructs a wait-for graph and determines whether $S'$ results in a failure, i.e., whether it contains a deadlock cycle, and returns the outcome $r$ (Line 6). If $r$ is marked as *Fail*, the scenario $S'$ is added to the DLS set $\mathbf{F}$ (Lines 7-8). If no failure is detected, *Conflict Feedback* evaluates the scenario $S'$ by computing a feedback score $\phi_{S'}$, which reflects the degree of spatial conflicts and temporal interaction among the AV group (Lines 9-10). If $\phi_{S'} < \phi_S$, the new seed $S'$ is retained in the corpus $\mathbf{Q}$ (Lines 11-12), indicating that $S'$ has a higher potential to evolve into a deadlock scenario compared to the original seed. The process repeats until the time limit is reached, after which the final set of detected DLSs $\mathbf{F}$ is returned (Line 14).

## 4.2 *Deadlock Oracle*

As defined in Definition 3.2, a deadlock is identified by detecting a scene $\mathbf{o}_t$ whose wait-for graph $G_t = (\mathcal{V}, \mathcal{E}_t)$ exists a cycle $(AV_{i_1}, e_t^{i_1 \to i_2}, AV_{i_2}, e_t^{i_2 \to i_3}, AV_{i_3}, \ldots, AV_{i_k}, e_t^{i_k \to i_1}, AV_{i_1})$.

Therefore, given a scenario observation $O(S)$, we need to extract the corresponding Wait-for Graph for each time, with a particular focus on identifying the wait-for edges associated with each AV. However, given a scenario observation, we can only access low-level outputs of the ADS, such as trajectories and vehicle states, which makes it challenging to infer high-level wait-for intentions. To address this, given an autonomous vehicle $\mathrm{AV}_i$, we estimate its wait-for edge $e_{i \to j}$ with respect to another vehicle $\mathrm{AV}_j$ by evaluating whether the following condition holds:

$$\Phi_{\text{edge}}(e_{i \to j}) = \Phi_{\text{stop}}(\mathrm{AV}_i) \wedge \Phi_{\text{intent}}(\mathrm{AV}_i, \mathrm{AV}_j)$$

Here, $\Phi_{\text{stop}}$ determines whether $\mathrm{AV}_i$ is in a stationary state, and $\Phi_{\text{intent}}$ predicts whether $\mathrm{AV}_j$ is likely to move into the intended path of $\mathrm{AV}_i$, thereby preventing it from proceeding.

The first condition $\Phi_{\text{stop}}$ can be easily determined by monitoring the speed of the vehicle by:

$$\Phi_{\text{stop}}(\mathrm{AV}_i) = \begin{cases} \texttt{True}, & \text{if } v_i(t') < \epsilon,\ \forall t' \in [t_i^{stop} + \Delta t, t_i^{stop}] \\ \texttt{False}, & \text{otherwise} \end{cases}$$

where $v_i(t')$ denotes the speed of $\mathrm{AV}_i$ at time $t'$, $\epsilon$ is a small velocity threshold (e.g., 0.01 m/s), and $\Delta t$ is the minimum duration for which the AV must remain below this threshold to be considered stationary.

To evaluate the second condition $\Phi_{\text{intent}}$, we examine whether there is an intention conflict between $\mathrm{AV}_i$ and $\mathrm{AV}_j$ during the time interval $[t_i^{\text{stop}} - \Delta t,\ t_i^{\text{stop}}]$, where $t_i^{\text{stop}}$ denotes the time at which $\mathrm{AV}_i$ comes to a complete stop. Specifically, given historical motion observations, we first predict the intended trajectory of $\mathrm{AV}_i$ over the pre-stop interval, denoted by $\tau_i^{\text{pre}}$, and the future trajectory of $\mathrm{AV}_j$, denoted by $\tau_j^{\text{pred}}$, using a Kalman Filter-based prediction approach [13, 34, 67]. Then, the condition $\Phi_{\text{intent}}$ is evaluated as follows:

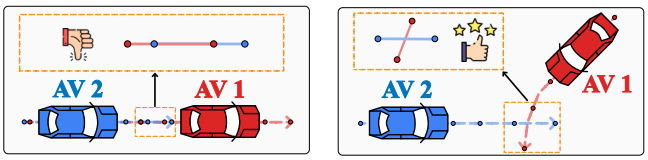
$$\Phi_{\text{intent}}(\mathrm{AV}_i, \mathrm{AV}_j) = \begin{cases} \texttt{True}, & \text{if Conflict}(\tau_i^{\text{pre}}, \tau_j^{\text{pred}}) = \texttt{True} \\ \texttt{False}, & \text{otherwise} \end{cases}$$

Here, $\text{Conflict}(\tau_i^{\text{pre}}, \tau_j^{\text{pred}})$ returns True if the two sets of trajectories overlap in both space and time, suggesting a potential interaction that may have contributed to $\mathrm{AV}_i$'s decision to stop.

Finally, by iterating over all autonomous vehicles in $\mathcal{A}$ and evaluating the condition $\Phi_{\text{edge}}(e_{i \to j})$ for each vehicle pair, we construct the complete wait-for graph $G$. A deadlock can then be detected by checking whether $G$ contains at least one cycle, i.e., $\Phi_{\text{cycle}}(G) = \texttt{True}$.

## 4.3 *Conflict Feedback*

The feedback component aims to effectively guide the generation of scenarios that are likely to induce mutual exclusion conditions. For example, if two ego vehicles have intersecting conflict regions




**(a) Non Spatial Conflict Region** **(b) Spatial Conflict Region**

**Figure 3: Illustration of spatial conflict regions.**

in their planned trajectories, a deadlock is more likely to occur. In addition to spatial factors, temporal attributes are also critical. The vehicles should approach the conflict region simultaneously or within a short time window to increase the likelihood of triggering a deadlock. Therefore, we design the feedback by considering two complementary aspects: (1) the *Spatial-Conflict Score*, which captures the spatial conflict relationships among AVs' trajectories; and (2) the *Temporal-Conflict Score*, which reflects the temporal competitiveness between AVs that are near conflict regions.

*4.3.1 Spatial-Conflict Score.* Given a scenario observation $O(S)$, we compute the spatial conflict point set $C_S$, defined as the set of pairwise intersections between trajectory segments, excluding fully overlapping cases. Specifically, the observed trajectory of $\text{AV}_i$ is represented as a sequence of line segments $\tau_S^i = \{\ell_{i,k} \mid k = 1, \ldots, N_i - 1\}$, where $N_i$ is the number of trajectory points, and each segment $\ell_{i,k} = (\mathbf{p}_{i,k}, \mathbf{p}_{i,k+1})$ connects two consecutive points. Here, $\mathbf{p}_{i,k} \in \mathbb{R}^2$ denotes the $k$-th spatial point on the trajectory of $\text{AV}_i$. We consider two segments $\ell_{i,k}$ and $\ell_{j,m}$ to be in spatial conflict if they intersect geometrically and are not aligned in the same direction. As illustrated in Fig. 3(a), when AV 1 follows AV 2 along an identical path segment with the same direction, the leading vehicle is unlikely to wait for the following vehicle, as they are not competing for the same conflict region. In contrast, Fig. 3(b) demonstrates a case where the two AVs approach the same region from different directions, increasing the likelihood of wait-for behavior due to mutual spatial contention. Formally, a conflict is recorded if:

$$\ell_{i,k} \cap \ell_{j,m} \neq \emptyset \quad \text{and} \quad ID(\ell_{i,k}) \neq ID(\ell_{j,m}),$$

where $ID(\ell_{i,k})$ denotes the ID the of the lane that $\ell_{i,k}$) belongs to. This ensures that non-competitive interactions such as following or coasting in the same direction are not counted as spatial conflicts. The total number of such conflict points, denoted as $|C_S|$, provides a measure of the spatial conflict degree in scenario $S$. This value is normalized with respect to the total number of trajectory segments across all AVs and is used as the spatial component of the feedback score:

$$\phi_S^{\text{spatial}} = 1 - \frac{|C_S|}{\sum_{i=1}^{|\mathcal{A}|}(N_i - 1)}.$$

A lower value of $\phi_S^{\text{spatial}} \in [0, 1]$ indicates that scenario $S$ exhibits stronger spatial competition, with more frequent trajectory intersections among AVs, suggesting a higher likelihood of potential deadlocks.

*4.3.2 Temporal-Conflict Score.* For each conflict region $R \in C_S$, where $C_S$ is the conflict point set obtained in the previous step, we directly estimate the arrival time $t_R^{\text{AV}_i}$ and speed $v_R^{\text{AV}_i}$ for each vehicle $\text{AV}_i$ that passes through region $R$, based on the scenario observation $O(S)$. These values can be obtained by identifying the scene timestamp at which the vehicle is closest to the conflict region. Therefore, for each conflict region $R \in C_S$, we compute a temporal conflict score $\phi_R$ as:

$$\phi_R = \min_{\substack{i,j \in \mathcal{A}_R \\ i \neq j}} \left( \left| t_R^i - t_R^j \right| + v_R^i + v_R^j \right),$$

where $\mathcal{A}_R$ denotes the set of AVs that pass through the conflict region $R$, $t_R^i$ is the estimated arrival time of $\text{AV}_i$, and $v_R^i$ is its corresponding speed at region $R$. This score captures the temporal proximity and velocity of competing AVs at the same region, with lower values indicating stronger temporal competition. Then, the final temporal-conflict score for scenario $S$ is computed as the minimum conflict score across all conflict regions, normalized into the range $[0, 1]$:

$$\phi_S^{\text{temporal}} = \text{clip}\left( \frac{\min_{R \in C_S} \phi_R}{N_{\text{ti}}},\ 0,\ 1 \right),$$

where $N_{\text{temporal}}$ is a scaling factor used to normalize the score. A lower value of $\phi_S^{\text{temporal}}$ indicates tighter temporal overlap and stronger competition among AVs at spatial conflict regions, particularly at lower speeds, suggesting a higher potential for wait-for behaviors and deadlocks.

*4.3.3 Overall Feedback Score.* Finally, the overall feedback score $\phi_S \in [0, 1]$ for a given scenario $S$ is calculated as:

$$\phi_S = \alpha \phi_S^{\text{spatial}} + (1 - \alpha) \phi_S^{\text{temporal}}$$

which combines the spatial-conflict score $\phi_S^{\text{spatial}}$ and the temporal conflict score $\phi_S^{\text{temporal}}$. The weighting factor $\alpha \in [0, 1]$ balances the contribution of each component. *STCLocker* aims to minimize $\phi_S$, thereby guiding the scenario generation process toward cases that are more likely to induce deadlocks.

## 4.4 *Conflict-aware Scenario Generation*

To improve the testing performance of *STCLocker*, we need to design scenarios where the AVs have shared regions and arrive at the shared regions simultaneously. Therefore, we design *Conflict-aware Scenario Generation* with two key components: *Temporal-aware Mutation* and *Spatial-aware Mutation*. These components aim to effectively improve feedback scores (both spatial and temporal) by guiding mutations toward promising directions, rather than relying on arbitrary mutations that often yield low scores.

The *Temporal-aware Mutation* adjusts fine-grained attributes of AVs, mainly their start times or initial delays, aiming to encourage the AVs to arrive the shared regions simultaneously. The *Spatial-aware Mutation*, on the other hand, aims to generate new scenarios with more conflict regions among AVs by altering their initial positions, routes, or spawn locations to promote topological convergence.

Algorithm 2 outlines the scenario generation process, which takes as input the parent scenario $S$, its feedback score $\phi_S$, and the corresponding conflict point set $C_S$, and returns a newly generated scenario $S'$ (Lines 5-6). Overall, the generation process first attempts a fine-grained **`TemporalMutation`** (Lines 7-16) to adjust timing attributes of AVs (Line 2). If the temporal mutation returns an

**Algorithm 2:** Algorithm of Scenario Generation

**Input** : Scenario $\mathcal{S} = \{\mathcal{A}, \mathcal{P}\}$
Feedback score $\phi_S$
Conflict points set $C_S$
**Output** : Mutated scenario $S' = \{\mathcal{A}', \mathcal{P}'\}$
**Parameters**: Maximum AV Capability $N_{\mathcal{A}}$
Local search bugdet $N_{local}$

1 **Function** `ScenarioGeneration`():
2 $\mathcal{A}' \leftarrow$ `TemporalMutation`$(\mathcal{A}, C_S)$
3 **if** $\mathcal{A}' = \emptyset \vee random() < \phi_S$ **then**
4 $\mathcal{A}', \mathcal{P}' \leftarrow$ `SpatialMutation`$(\mathcal{A})$
5 $S' \leftarrow \{\mathcal{A}', \mathcal{P}'\}$
6 **return** $S'$
7 **Function** `TemporalMutation`$(\mathcal{A}, C_S)$:
8 **if** $|C_S| = \emptyset$ **then**
9 **return** $\emptyset$
10 $\mathcal{A}' \leftarrow \mathcal{A}$ // Copy $\mathcal{A}$ to $\mathcal{A}'$
11 $R \leftarrow$ RandomSelect$(C_S)$
12 **for** $(AV_i, AV_j) \in RandomPair(\mathcal{A}_R)$ **do**
13 $\Delta t'_R \leftarrow t_R^{\mathrm{AV}_i} - t_R^{\mathrm{AV}_j}$
// Update trigger time in $\mathcal{A}'$
14 $t'^{trigger}_i = \max\{0, t_i^{trigger} - \frac{\Delta t'_R}{2}\}$
15 $t'^{trigger}_j = \max\{0, t_j^{trigger} + \frac{\Delta t'_R}{2}\}$
16 **return** $\mathcal{A}'$
17 **Function** `SpatialMutation`$(\mathcal{A})$:
18 $\mathcal{A}' \leftarrow \mathcal{A}$ // Copy $\mathcal{A}$ to $\mathcal{A}'$
19 **if** $|\mathcal{A}'| \geq N_{\mathcal{A}}$ **then**
20 $\mathcal{A}' \leftarrow$ RandomRemove$(\mathcal{A}', \min = 0, \max = N_{\mathcal{A}} - 2)$
// Local search best config
21 $\mathrm{AV}_{best} \leftarrow$ RandomCreate()
22 $\phi^{\mathrm{spatial}}_{best} \leftarrow$ SpatialScore$(\mathbf{Q}, \mathcal{A}' \cup \{\mathrm{AV}_{best}\})$
23 **for** $i < N_{local}$ **do**
24 $\mathrm{AV}_{tmp} \leftarrow$ RandomCreate()
25 $\phi^{\mathrm{spatial}}_{tmp} \leftarrow$ SpatialScore$(\mathcal{A}' \cup \{\mathrm{AV}_{tmp}\})$
26 **if** $\phi^{spatial}_{tmp} < \phi^{spatial}_{best}$ **then**
27 $\phi^{\mathrm{spatial}}_{best} \leftarrow \phi^{\mathrm{spatial}}_{tmp}$
28 $\mathrm{AV}_{best} \leftarrow \mathrm{AV}_{tmp}$
29 $\mathcal{A}' \leftarrow \mathcal{A}' \cup \{\mathrm{AV}_{best}\}$
// Mutate NPC participants
30 $\mathcal{P}' \leftarrow$ WaypointMutator$(\mathcal{P})$
31 **return** $\mathcal{A}', \mathcal{P}'$

empty set, indicating that the parent scenario contains no conflict regions as determined in Lines 9-10, the process falls back to a spatial mutation (Lines 3-4). Additionally, if the feedback score $\phi_S$ is too high, indicating weak spatial-temporal interactions, the generation process will have a high probability of selecting the **`SpatialMutation`** in order to explore alternative spatial conflict patterns.

*4.4.1 Temporal-aware Mutation.* Given a set of AVs $\mathcal{A}$ and their corresponding conflict point set $C_S$, the temporal mutation aims to adjust the trigger times of vehicles in $\mathcal{A}$ to enhance inter-vehicle

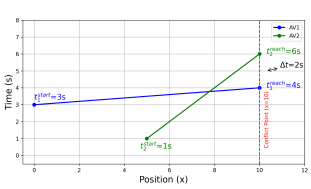



**Figure 4: Original scenario.**

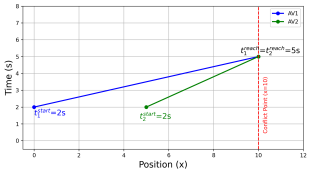



**Figure 5: After temporal-aware mutation.**

competitive interactions (Lines 7-16). Specifically, a new set $\mathcal{A}'$ is first initialized as a copy of $\mathcal{A}$ (Line 10). The algorithm then randomly selects a conflict region $R \in C_S$ and iteratively adjusts the trigger times of the set of AVs that pass through region $R$, denoted as $\mathcal{A}_R$ (Lines 11–15). For each pair $(\mathrm{AV}_i, \mathrm{AV}_j) \in \mathcal{A}_R$, their trigger times are modified to reduce the arrival time gap at $R$, thereby promoting simultaneous access to the shared region (Lines 12-15). To increase the likelihood of interaction, we temporally adjust the triggering time of both AVs, by the following rule:

$$t_i'^{\mathrm{trigger}} = \max\left\{0,\ t_i^{\mathrm{trigger}} - \frac{\Delta t'_R}{2}\right\},$$

where $\Delta t'_R$ denotes the relative temporal offset between the two AVs at the conflict region. This adjustment aims to synchronize their arrival times so that they reach the conflict point simultaneously in the mutated scenario. Figs. 4 and 5 illustrate the original scenario and the scenario after temporal-aware mutation. Mutated set $\mathcal{A}'$ is returned (Line 16).

*4.4.2 Spatial-aware Mutation.* To prevent the search process from getting stuck in fine-grained optimization within the roads of the current scenarios, we also explore alternative and more competitive spatial conflict configurations among AVs. Specifically, given an AV set $\mathcal{A}$, the spatial mutation begins by initializing a mutated set $\mathcal{A}'$ as a copy of $\mathcal{A}$ (Line 18). To maintain scenario complexity within reasonable bounds, if the number of AVs exceeds a predefined capacity $N_{\mathcal{A}} (\geq 3)$, a random subset of size $n \in [1, N_{\mathcal{A}} - 2]$ is removed (Lines 19-20). This ensures that at least two AVs remain to support meaningful multi-AV interactions. Next, the spatial mutation performs an offline local search with a maximum of $N_{\mathrm{local}}$ iterations to identify a new AV configuration that yields a relatively lower estimated spatial-conflict score (Lines 21-28). The search begins by randomly initializing a new AV configuration $\mathrm{AV}_{\mathrm{best}}$, and computing its spatial-conflict score $\phi^{\mathrm{spatial}}_{\mathrm{best}}$ using the SpatialScore function (Line 22), as detailed in Section 4.3.1. Since the scenario is not executed during this stage, the trajectory of each newly generated AV $\mathrm{AV}_{\mathrm{tmp}}$ can be estimated using the path planning algorithms applied in the current ADSs, such as the A* algorithm [61] used in Apollo, Autoware and Roach, based on a start point, destination point, and the road map. In each local search iteration, a new AV configuration $\mathrm{AV}_{\mathrm{tmp}}$ is randomly sampled (Line 26), and $\mathrm{AV}_{\mathrm{best}}$ is updated if $\mathrm{AV}_{\mathrm{tmp}}$ achieves a lower spatial-conflict score (Lines 23-28). The best configuration $\mathrm{AV}_{\mathrm{best}}$ is then selected and incorporated into the scenario to form the mutated AV set $\mathcal{A}'$ (Line 29).

In addition, we apply a waypoint mutator [8, 28, 35, 64] to perturb other non-player character (NPC) participants in the scenario, introducing additional variability and diversity (Line 30). Note that the perturbations are constrained to regions that do not conflict with

the AVs, in order to preserve the integrity of the targeted multi-AVs interactions and avoid introducing unintended interference.

Finally, the mutated AV set $\mathcal{A}'$ and the participant set $\mathcal{P}'$ are combined to form the new scenario $S' = \{\mathcal{A}', \mathcal{P}'\}$, which is returned for further execution and validation (Lines 5-6).

## 5 Evaluation Results

In this section, we aim to empirically evaluate the capability of *STCLocker* on generating (DLSs) for ADSs. In particular, we will answer the following research questions:

**RQ1:** Can *STCLocker* effectively generate DLSs for ADSs in multi-vehicle scenarios compared to baselines?

**RQ2:** What are the individual contributions of each component in *STCLocker* to its overall effectiveness?

**RQ3:** How does *STCLocker* perform in terms of testing time efficiency?

**Environment.** We performed our experiments using the high-fidelity CARLA simulator [11], evaluating two autonomous driving systems (ADSs): *Roach* [48] and *OpenCDA* [68]. *Roach* is a state-of-the-art end-to-end ADS that directly maps perception outputs to control commands for ego vehicle navigation. In contrast, *OpenCDA* is a modular ADS framework that incorporates cooperative mechanisms among multiple autonomous vehicles. Both systems are fully compatible with the CARLA simulation platform. In this paper, our primary objective is to evaluate the decision-making capabilities of ADSs. Therefore, following prior studies [8, 29, 52], we use ground-truth perception results obtained directly from the simulator to eliminate the influence of perception errors caused by algorithmic inaccuracies or just simulator-induced delays.

**Driving Scenarios.** We evaluate *STCLocker* on four representative driving map regions derived from the NHTSA pre-crash typology [40], which is widely adopted in prior ADS testing research [8, 29, 35, 64]. These regions reflect diverse real-world traffic scenarios that challenge decision-making under multi-vehicle interactions:

- *M1: CityRoad Intersection*, a four-way intersection, requiring AVs to handle yielding, turning.
- *M2: CityRoad T-Junction*, a T-shaped junction where AVs must perform merging or unprotected turns.
- *M3: Roundabout*, a circular intersection where AVs must coordinate entry, yielding, and exit.
- *M4: Highway Merging*, a highway segment with merging lanes, where AVs must safely enter traffic streams.

Different from prior testing approaches that rely on fixed route paths for autonomous vehicles (AVs), in this paper, we automatically determine and select both the start point and destination for each AV within the scenario's map region.

**Baselines.** To the best of our knowledge, this is the first work to conduct deadlock testing on ADSs, and thus no existing method serves as a direct baseline for comparison. Therefore, we compare *STCLocker* against two representative baselines: (1) *Random* and (2) *DoppelTest* [29]. Specifically, (1) *Random* does not incorporate any feedback or specific mutation strategies. It generates scenarios by randomly deploying AVs and NPC participants with arbitrary configurations. (2) *DoppelTest* is the only publicly available tool that supports testing with multiple autonomous vehicles. It uses a genetic algorithm guided by multiple safety-critical objectives such as inter-vehicle distance. Although originally designed for the Apollo and SimControl [3], we reuse its core algorithms to CARLA without modifying the core testing logic.

**Table 1: Comparison Results with Baselines on OpenCDA.**

| ADS | Method | #DLS (#DLS-Hum)↑ | | | | |
|---|---|---|---|---|---|---|
| | | *M1* | *M2* | *M3* | *M4* | *Sum.* |
| *Roach* | *Random* | 1.4 (0.6) | 3.2 (2.8) | 0.8 (0.8) | 2.2 (1.2) | 7.6 (5.4) |
| | *DoppelTest* | 2.8 (2.2) | 2.4 (2.4) | 0.8 (0.2) | 0.2 (0.2) | 6.2 (5.0) |
| | *STCLocker* | **14.0 (8.0)** | **24.2 (21.0)** | **11.6 (7.0)** | **15.6 (10.4)** | **65.4 (46.4)** |
| *OpenCDA* | *Random* | 7.0 (4.2) | 5.6 (2.4) | 5.6 (3.4) | 19.8 (11.8) | 38.0 (21.8) |
| | *DoppelTest* | 6.6 (4.2) | 17.2 (7.4) | 6.2 (2.6) | 22.6 (16.2) | 52.6 (29.2) |
| | *STCLocker* | **28.4 (14.0)** | **34.0 (10.6)** | **9.8 (4.0)** | **50.6 (19.6)** | **122.8 (48.2)** |

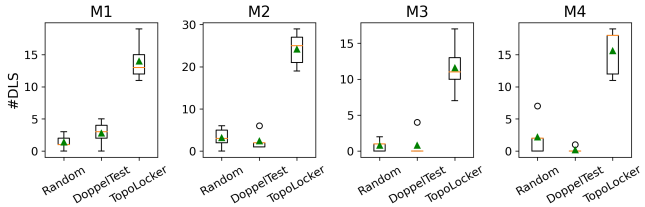



**Figure 6: Statistical comparison of #DLS on Roach.**

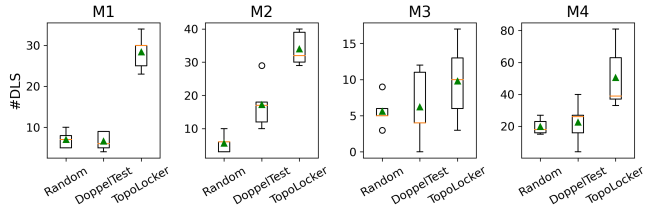



**Figure 7: Statistical comparison of #DLS on OpenCDA.**

**Metrics.** To enable a fair comparison with baseline techniques, we integrate our *Deadlock Oracle* into each of them to uniformly detect and collect generated DLSs. In our experiments, we evaluate the effectiveness of DLS generation using one primary metric, #DLS, which denotes the number of potential deadlock scenarios identified by *STCLocker*. In addition, we manually reviewed the simulation recordings corresponding to the detected DLSs. The number of deadlocks confirmed through human inspection is reported as #DLS-Hum.

**Implementation.** Similar to previous work [29], we set the maximum AV capacity $\mathcal{N}_{\mathcal{A}}$ around 6. We empirically set the oracle detection window $\Delta_t$ to 5 seconds based on preliminary observations. The weighting factor $\alpha$ is set to 0.5. Each experiment is repeated five times, and we report the average results across runs. For all methods, we allocate a fixed testing budget of two hours per run, which we found adequate for meaningful comparison. All experiments are conducted on a platform equipped with an AMD EPYC 9554P CPU, an NVIDIA L40 GPU, and 512GB of RAM. The experiments takes more than 30 GPU days in total.

### 5.1 RQ1: Effectiveness of *STCLocker*

*5.1.1 Comparative Results.* Table 1 compares #DLS and #DLS-Hum across four initial driving scenarios: *M1*, *M2*, *M3*, and *M4*, on two different types of ADSs: *Roach* and *OpenCDA*. Fig. 6 and Fig. 7 illustrate the distribution of #DLS across five repeated runs of each method in every scenario, where the orange bar represents the

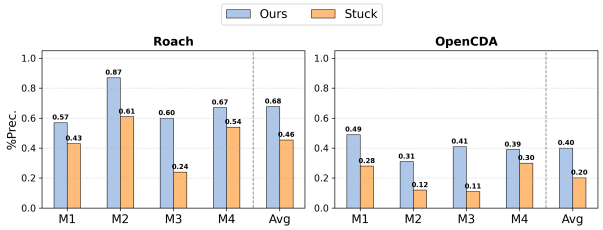



**Figure 8: Precision of oracles.**

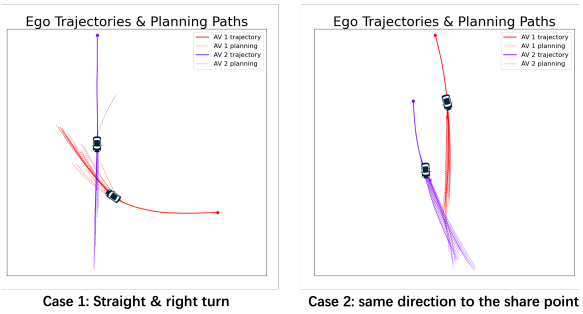



**Figure 9: Case Study of Deadlock Scenarios (DLSs). Solid lines represent execution paths, and dashed lines indicate predicted motion trajectories.**

median and the green triangle indicates the average. Overall, we find that *STCLocker* outperforms all baselines in both #DLS and #DLS-Hum across different ADSs and scenarios.

*Roach.* For the end-to-end ADS *Roach*, *STCLocker* achieves the best overall performance, significantly outperforming the best baseline (i.e., *Random*) with 65.4 vs. 7.6 detected #DLS cases. In detail, *STCLocker* surpasses the baseline in all scenarios: *M1* (14.0 vs. 1.4), *M2* (24.2 vs. 3.2), *M3* (11.6 vs. 0.8), and *M4* (15.6 vs. 2.2). Among the 65.4 deadlock cases detected by *STCLocker*, 46.4 were manually confirmed as valid deadlocks (#DLS-Hum), including 8.0 in *M1*, 21.0 in *M2*, 7.0 in *M3*, and 10.4 in *M4*. In contrast, the best-performing baselines achieved only 5.4 (*Random*) and 5.0 (*DoppelTest*) confirmed #DLS-Hum cases.

*OpenCDA.* For the modular ADS *OpenCDA*, which incorporates cooperative communication mechanisms, *STCLocker* also demonstrates clear advantages over the baselines. It achieves the highest values for both #DLS and #DLS-Hum across all four scenarios. Specifically, *STCLocker* outperforms the best baseline (i.e., *DoppelTest*) in *M1* (28.4 vs. 6.6), *M2* (34.0 vs. 17.2), *M3* (9.8 vs. 6.2), and *M4* (50.6 vs. 22.6). Manual inspection confirms 48.2 valid deadlock cases (#DLS-Hum). These results highlight *STCLocker*'s effectiveness in uncovering challenging multi-AV coordination failures, even in systems equipped with communication and cooperative mechanisms.

*Discussion.* By comparing the overall performance across both ADSs, we observe that fewer deadlocks occur in the *M3* Roundabout scenario. This is primarily because roundabouts are relatively rare and less familiar environments for both ADSs, which often struggle to handle them effectively. Such unfamiliarity can lead to safety-critical issues or cause the AVs to become stuck without recognizing viable navigational goals. Additionally, when comparing the overall performance of *Roach* and *OpenCDA*, we find that *Roach*, trained using reinforcement learning, surprisingly demonstrates better cooperative behavior by inducing fewer DLSs than *OpenCDA* (65.4 vs. 122.8 DLSs detected by *STCLocker*). A possible explanation is that the cooperative communication and fusion mechanisms in *OpenCDA*, being rule-based, lack generalizability and are highly sensitive to the execution order of decisions among ADSs. This makes the system more prone to coordination failures under unfamiliar or adversarial traffic conditions.

*5.1.2 Effectiveness of Deadlock Oracle.* To evaluate the effectiveness of *Deadlock Oracle*, we compare its detection performance against a naive variant that replaces *Deadlock Oracle* in *STCLocker* with a simple time-based counter for monitoring stuck behavior. Fig. 8 illustrates the precision of both oracles, computed as: %Prec. $= \frac{\#\text{DLS-Hum}}{\#\text{DLS}}$, which represents the proportion of automatically detected deadlocks that are confirmed through manual inspection. We observe that our proposed *Deadlock Oracle* significantly outperforms the naive time-based oracle, achieving 68% vs. 46% on *Roach*, and 40% vs. 20% on *OpenCDA*. These results demonstrate that simply detecting stuck behavior is insufficient to capture intention-driven wait-for cycles. They also highlight the effectiveness and necessity of our *Deadlock Oracle* for accurate deadlock detection in multi-AV scenarios.

*5.1.3 Case Study.* Fig. 9 shows representative DLS examples. These cases demonstrate how groups of AVs may fail to coordinate access to shared resources, leading to wait-for states that ultimately result in deadlocks.

*Case 1:* In this scenario, two vehicles, AV1 and AV2, are controlled by Roach to navigate an intersection where AV1 intends to make a right turn while AV2 proceeds straight. As shown in Fig. 9, both AVs become stuck in a deadlock at the approaching point. During the pre-stop interval, their predicted motion intentions (dash lines) exhibit dense spatial-temporal conflicts, indicating a high likelihood of mutual obstruction.

*Case 2:* This case illustrates a highway merging scenario involving two vehicles, AV1 and AV2, controlled by *OpenCDA*. AV2 slows down to join the platoon led by AV1, while AV1 simultaneously reduces its speed to avoid AV2's motion, which exhibits a high degree of intention overlap with AV1's predicted trajectory. This mutual hesitation results in a deadlock.

**Answer to RQ1**: *STCLocker* significantly outperforms existing methods in identifying DLSs under multi-vehicle autonomous driving scenarios.

## 5.2 RQ2: Usefulness of Components

We evaluated the key components of *STCLocker*'s testing process, including the *Conflict-aware Scenario Generation* and *Conflict Feedback*, by configuring a series of variants.

*5.2.1 Mutation.* For the mutation component, we compared *STCLocker* with two of its ablated variants: (1) *w/o Temporal* removes the temporal-aware mutation from *Conflict-aware Scenario Generation*, aiming to evaluate the benefits of temporal adjustments in generating deadlock scenarios; (2) *w/o Spatial* removes the spatial-aware mutation, allowing scenarios to be generated solely by adjusting

**Table 2: Effectiveness of mutation (top) and feedback (bottom).**

**(a) Mutation Strategies**

| ADS | Method | *M1* | *M2* | *M3* | *M4* | *Sum.* |
|---|---|---|---|---|---|---|
| *Roach* | *w/o Temporal* | 8.6 | 14.0 | 5.6 | 9.2 | 37.4 |
| | *w/o Spatial* | 11.0 | 15.6 | 9.2 | 10.6 | 46.4 |
| | *STCLocker* | **14.0** | **24.2** | **11.6** | **15.6** | **65.4** |
| *OpenCDA* | *w/o Temporal* | 23.0 | 27.4 | 9.0 | 40.0 | 99.4 |
| | *w/o Spatial* | 32.4 | 30.0 | 6.2 | 46.0 | 114.6 |
| | *STCLocker* | **28.4** | **34.0** | **9.8** | **50.6** | **122.8** |

**(b) Feedback Variants**

| ADS | Method | *M1* | *M2* | *M3* | *M4* | *Sum.* |
|---|---|---|---|---|---|---|
| *Roach* | *f-Random* | 5.0 | 8.6 | 3.2 | 2.0 | 18.8 |
| | *f-Spatial* | 9.0 | 11.4 | 6.0 | 12.2 | 38.6 |
| | *f-Temporal* | 11.4 | 12.6 | 4.0 | 7.2 | 35.2 |
| | *STCLocker* | **14.0** | **24.2** | **11.6** | **15.6** | **65.4** |
| *OpenCDA* | *f-Random* | 16.8 | 18.0 | 5.6 | 23.4 | 55.2 |
| | *f-Spatial* | 19.0 | 29.0 | 5.2 | 23.4 | 76.6 |
| | *f-Temporal* | 25.4 | 27.0 | 5.6 | 39.0 | 97.0 |
| | *STCLocker* | **28.4** | **34.0** | **9.8** | **50.6** | **122.8** |

the trigger times of ego vehicles. This variant is designed to assess the effectiveness of spatial conflicts in mutation.

Table 2 (a) presents the comparison results. We observe that removing either component (*w/o Temporal* or *w/o Spatial*) results in fewer DLSs generated compared to the full version of *STCLocker* across both ADSs. Notably, *w/o Temporal* produces the fewest DLS, with 37.4 on *Roach* and 99.4 on *OpenCDA*, demonstrating that temporal-aware mutation (i.e., via trigger time adjustment) is particularly effective in uncovering deadlocks. This effectiveness stems from the fact that fine-grained timing modifications directly affect the concurrency of AV behaviors at conflict regions, thereby increasing the likelihood of simultaneous contention and deadlock formation. In addition, *w/o Spatial* also results in performance drops when the spatial-aware mutation is removed: the number of DLSs drops from 65.4 to 46.4 on *Roach*, and from 122.8 to 114.6 on *OpenCDA*. This illustrates that spatial mutation contributes by introducing topological conflicts, enabling more competitive configurations to emerge. Overall, these results demonstrate the complementary contributions of both mutation strategies and highlight the importance of jointly incorporating spatial and temporal mutation to effectively generate deadlock scenarios.

*5.2.2 Feedback.* For the feedback component, we implemented three variants to evaluate its effectiveness: (1) *f-Random* replaces the feedback mechanism in *STCLocker* with random selection, meaning that both seed scenarios and mutation selection are chosen randomly. This variant serves as a baseline to assess the overall value of guided feedback; (2) *f-Spatial* relies solely on the *Spatial-Conflict Score* to evaluate its individual contribution; (3) *f-Temporal* uses only the *Temporal-Conflict Score* to assess its role in guiding the search.

Table 2 (b) shows the experimental results in terms of the number of DLSs discovered. The comparison between *f-Random* and *STCLocker* (18.8 vs. 65.4 on *Roach*, and 55.2 vs. 122.8 on *OpenCDA*) illustrates the effectiveness of feedback-guided search in *STCLocker*.

**Table 3: Result of time performance (second).**

| Method | Mutation | Oracle | Feedback | Simulation | Total |
|---|---|---|---|---|---|
| *Random* | 3.99 | N/A | N/A | 52.87 | 56.86 |
| *DoppelTest* | 4.18 | 0.08 | 0.37 | 45.27 | 49.90 |
| *STCLocker* | 7.62 | 0.72 | 1.18 | 61.89 | 71.41 |

Note that *f-Random* outperforms *Random*, which highlights the contribution of the *Conflict-aware Scenario Generation* component even in the absence of any feedback guidance. Moreover, the results of *f-Spatial* (38.6 on *Roach*, 76.6 on *OpenCDA*) and *f-Temporal* (35.2 on *Roach*, 97.0 on *OpenCDA*) demonstrate that both the spatial and temporal feedback contribute meaningfully to deadlock detection. Their combination achieves the best performance.

**Answer to RQ2**: Both the spatial and temporal designs in the mutation and feedback components are essential for enabling *STCLocker* to effectively generate deadlock scenarios.

## 5.3 RQ3: Testing Performance

We further assess the time performance of the main components in *STCLocker*, including the overhead introduced by mutation, oracle checking, feedback computation, and simulation execution. Specifically, we analyze the average time required to process a single scenario. The results are summarized in Table 3, where the columns *Mutation*, *Oracle*, *Feedback*, and *Simulation* report the average time (in seconds) spent on each corresponding stage: applying mutations, performing oracle checks, computing feedback scores, and running the scenario in the simulation platform. For the *Random* variant, the oracle and feedback stages are not applicable and are marked as 'N/A'.

Overall, the results show that simulation dominates the total processing time in all methods. For example, on average, *STCLocker* takes 71.41 seconds to process a single scenario, of which 61.89 seconds (86.7%) are spent on simulation. This higher simulation time, compared to other approaches, is primarily due to the need to observe a prolonged stationary period for effective deadlock detection. In terms of testing components, *STCLocker* incurs slightly more time in mutation, oracle evaluation, and feedback processing, reflecting the additional computation required to guide the generation of deadlock-prone scenarios. The most time-consuming operations are the spatial conflict pre-checking in the spatial-aware mutation and the conflict region identification during feedback evaluation. Nevertheless, simulation time remains the dominant component of overall testing, and the additional overhead introduced by *STCLocker* has only a minor impact on total testing time and overall testing performance.

**Answer to RQ3**:*STCLocker* slightly increases the proportion of non-simulation computation time; however, the majority of the testing time is still dominated by simulation.

## 5.4 Threats to Validity

*STCLocker* faces several potential threats to validity. First, the choice of the autonomous driving systems (ADSs) under evaluation may influence the results. To mitigate this concern, we conducted experiments on two distinct types of ADSs that are widely used, well-evaluated, and stably compatible with the CARLA simulator. Since

our method is ADS-agnostic by design, it can be readily extended to other ADSs, which we plan to explore in future work. Second, our evaluation does not consider the effects of perception errors. As this paper focuses specifically on assessing the decision-making modules of ADSs, we follow prior work [8, 29, 52] in excluding perception-related noise, which could otherwise obscure the clarity of our analysis. Third, the accuracy of wait-for graph construction and the configuration of stationary period thresholds may pose potential threats to validity. In particular, inaccurate motion prediction could lead to incorrect intention inference, and premature classification of deadlocks may occur if ego vehicles eventually resume movement. To mitigate these risks, we manually reviewed each case and excluded those exhibiting significant prediction errors or false deadlock indications, ensuring the reliability of our analysis. Lastly, the diversity of driving scenarios and the inherent non-determinism in ADS execution may also pose threats to the validity of our results. To mitigate these factors, we select a wide range of different driving scenarios and repeat each experiment multiple times to account for stochastic variations.

## 6 Related Works

**ADS Testing.** As testing is critical for ensuring the safety and reliability of autonomous driving systems (ADS), the development of efficient and effective testing methodologies has garnered sustained attention from the research community. Broadly, existing approaches can be categorized into two major groups: data-driven testing [10, 15, 39, 41, 43, 44, 49, 71] and search-based testing [8, 23, 24, 29, 35, 55–58, 64, 74, 75]. *Data-driven testing* leverages real-world data sources to construct critical test scenarios. These sources include traffic logs [10, 44, 49, 54] and accident reports [15, 21, 41, 43, 53, 71], enabling the reproduction or simulation of historically risky driving behaviors. *Search-based testing*, on the other hand, explores the scenario space systematically to identify safety-critical cases. Techniques in this category include: guided fuzzing [8, 35, 45], evolutionary algorithms [16, 23, 56–58, 62, 75], metamorphic testing [22], surrogate model-guided search [24, 74], reinforcement learning [14, 25, 38], and reachability analysis [1, 26]. These methods have demonstrated their effectiveness in revealing vulnerabilities in ADS decision-making. However, most focus on either individual vehicle behavior or single-agent criticality, with limited attention paid to multi-agent interactions such as deadlock, a gap that our work seeks to address.

**Cooperative Autonomous Driving.** Cooperative autonomous driving is a paradigm in which two or more connected automated vehicles (CAVs) communicate and coordinate their actions to achieve their respective driving objectives [2]. This paradigm aims to enhance the efficiency, safety, and reliability of ADSs in complex traffic environments. Existing approaches to cooperative driving can be broadly classified into two categories. The first involves *decentralized cooperation*, where individual vehicles exchange information such as sensor data [59], perception results [33, 65], or planning outputs [69, 70]. This model enables vehicles to adapt their behavior in real time based on local observations and peer communications. However, it also introduces challenges related to communication reliability and the complexity of multi-source data fusion [17, 42]. The second category is *centralized coordination*, where a central controller (or master) plans and distributes decisions to all participating vehicles [6, 19]. While centralized systems offer more stable and globally optimized coordination, they typically suffer from limited adaptability and increased latency in dynamic environments. Although cooperative autonomous driving has gained growing attention, research on multi-vehicle collaboration remains relatively limited compared to the extensive work on individual ADSs [30]. In particular, the evaluation of failure modes such as coordination conflicts and deadlock scenarios has not been sufficiently explored. Our work also addresses this gap by systematically testing cooperative ADS behaviors under conditions that may lead to inter-vehicle deadlocks.

## 7 Conclusion

In this paper, we present the first study to evaluate the cooperative capabilities of ADSs, with a particular focus on their ability to handle deadlocks in multi-vehicle traffic scenarios. To address this challenge, we develop an effective testing tool, *STCLocker*, which integrates three key components: *Deadlock Oracle*, to accurately identify wait-for deadlock situations among multiple autonomous vehicles; *Conflict Feedback* and *Conflict-aware Scenario Generation*, which work collaboratively to guide the search process to discover more deadlock scenarios. Experimental results demonstrate the effectiveness and efficiency of *STCLocker*, as well as the contribution of each individual component.

## References


[1] Matthias Althoff and Sebastian Lutz. 2018. Automatic generation of safety-critical test scenarios for collision avoidance of road vehicles. In *2018 IEEE Intelligent Vehicles Symposium (IV)*. IEEE, Changshu, Suzhou, China, 1326–1333.

[2] Cooperative Driving Automation. 2020. *Taxonomy and definitions for terms related to cooperative driving automation for on-road motor vehicles.* SAE International.

[3] Baidu. 2019. Apollo: Open Source Autonomous Driving. https://github.com/ApolloAuto/apollo

[4] Baidu. 2025. Apollo Go. https://www.apollogo.com/. Accessed: May 2025.

[5] Rebecca Bellan. 2024. 6 Waymo robotaxis block traffic to San Francisco freeway on-ramp. *TechCrunch* (17 April 2024). https://techcrunch.com/2024/04/17/seven-waymo-robotaxis-block-traffic-to-san-francisco-freeway-on-ramp/ Accessed: May 31, 2025.

[6] Na Chen, Bart van Arem, Tom Alkim, and Meng Wang. 2021. A Hierarchical Model-Based Optimization Control Approach for Cooperative Merging by Connected Automated Vehicles. *IEEE Transactions on Intelligent Transportation Systems* 22, 12 (2021), 7712–7725. doi:10.1109/TITS.2020.3007647

[7] Mingfei Cheng, Xiaofei Xie, Yuan Zhou, Junjie Wang, Guozhu Meng, and Kairui Yang. 2025. Decictor: Towards Evaluating the Robustness of Decision-Making in Autonomous Driving Systems . In *2025 IEEE/ACM 47th International Conference on Software Engineering (ICSE)*. 651–651.

[8] Mingfei Cheng, Yuan Zhou, and Xiaofei Xie. 2023. BehAVExplor: Behavior Diversity Guided Testing for Autonomous Driving Systems. In *Proceedings of the 32nd ACM SIGSOFT International Symposium on Software Testing and Analysis*. 488–500.

[9] comma.ai. 2022. OpenPilot: An open source driver assistance system. Retrieved Nov 7, 2022 from https://github.com/commaai/openpilot

[10] Yao Deng, Xi Zheng, Mengshi Zhang, Guannan Lou, and Tianyi Zhang. 2022. Scenario-based test reduction and prioritization for multi-module autonomous driving systems. In *Proceedings of the 30th ACM Joint European Software Engineering Conference and Symposium on the Foundations of Software Engineering*. 82–93.

[11] Alexey Dosovitskiy, German Ros, Felipe Codevilla, Antonio Lopez, and Vladlen Koltun. 2017. CARLA: An Open Urban Driving Simulator. In *Proceedings of the 1st Annual Conference on Robot Learning (Proceedings of Machine Learning Research, Vol. 78)*, Sergey Levine, Vincent Vanhoucke, and Ken Goldberg (Eds.). PMLR, California, USA, 1–16.

[12] EDM.com Staff. 2024. Google's Self-Driving Waymo Cars Appear to Stall, Block Traffic Out of Portola Festival. *EDM.com* (2024). https://edm.com/news/google-

self-driving-waymo-cars-fail-block-traffic-portola-festival Accessed: May 31, 2025.

[13] Azadeh Emami, Majid Sarvi, and Saeed Asadi Bagloee. 2019. Using Kalman filter algorithm for short-term traffic flow prediction in a connected vehicle environment. *Journal of Modern Transportation* 27 (2019), 222–232.

[14] Shuo Feng, Haowei Sun, Xintao Yan, Haojie Zhu, Zhengxia Zou, Shengyin Shen, and Henry X Liu. 2023. Dense reinforcement learning for safety validation of autonomous vehicles. *Nature* 615, 7953 (2023), 620–627.

[15] Alessio Gambi, Tri Huynh, and Gordon Fraser. 2019. Generating effective test cases for self-driving cars from police reports. In *Proceedings of the 2019 27th ACM Joint Meeting on European Software Engineering Conference and Symposium on the Foundations of Software Engineering*. ACM, Tallinn Estonia, 257–267.

[16] Alessio Gambi, Marc Mueller, and Gordon Fraser. 2019. Automatically testing self-driving cars with search-based procedural content generation. In *Proceedings of the 28th ACM SIGSOFT International Symposium on Software Testing and Analysis*. ACM, Beijing, China, 318–328.

[17] Xin Gao, Xinyu Zhang, Yiguo Lu, Yuning Huang, Lei Yang, Yijin Xiong, and Peng Liu. 2024. A Survey of Collaborative Perception in Intelligent Vehicles at Intersections. *IEEE Transactions on Intelligent Vehicles* (2024), 1–20. doi:10.1109/TIV.2024.3395783

[18] Joshua Garcia, Yang Feng, Junjie Shen, Sumaya Almanee, Yuan Xia, and Qi Alfred Chen. 2020. A comprehensive study of autonomous vehicle bugs. In *Proceedings of the ACM/IEEE 42nd International Conference on Software Engineering*. IEEE, Seoul, South Korea, 385–396.

[19] Ashkan Gholamhosseinian and Jochen Seitz. 2022. A Comprehensive Survey on Cooperative Intersection Management for Heterogeneous Connected Vehicles. *IEEE Access* 10 (2022), 7937–7972. doi:10.1109/ACCESS.2022.3142450

[20] Ionel Gog, Sukrit Kalra, Peter Schafhalter, Matthew A Wright, Joseph E Gonzalez, and Ion Stoica. 2021. Pylot: A modular platform for exploring latency-accuracy tradeoffs in autonomous vehicles. In *2021 IEEE International Conference on Robotics and Automation (ICRA)*. IEEE, 8806–8813.

[21] An Guo, Yuan Zhou, Haoxiang Tian, Chunrong Fang, Yunjian Sun, Weisong Sun, Xinyu Gao, Anh Tuan Luu, Yang Liu, and Zhenyu Chen. 2024. Sovar: Build generalizable scenarios from accident reports for autonomous driving testing. In *Proceedings of the 39th IEEE/ACM International Conference on Automated Software Engineering*. 268–280.

[22] Jia Cheng Han and Zhi Quan Zhou. 2020. Metamorphic fuzz testing of autonomous vehicles. In *Proceedings of the IEEE/ACM 42nd International Conference on Software Engineering Workshops*. 380–385.

[23] Seunghee Han, Jaeuk Kim, Geon Kim, Jaemin Cho, Jiin Kim, and Shin Yoo. 2021. Preliminary evaluation of path-aware crossover operators for search-based test data generation for autonomous driving. In *2021 IEEE/ACM 14th International Workshop on Search-Based Software Testing (SBST)*. IEEE, Madrid, Spain, 44–47.

[24] Fitash Ul Haq, Donghwan Shin, and Lionel Briand. 2022. Efficient online testing for DNN-enabled systems using surrogate-assisted and many-objective optimization. In *Proceedings of the 44th International Conference on Software Engineering*. IEEE, Pittsburgh Pennsylvania, 811–822.

[25] Fitash Ul Haq, Donghwan Shin, and Lionel C Briand. 2023. Many-objective reinforcement learning for online testing of dnn-enabled systems. In *2023 IEEE/ACM 45th International Conference on Software Engineering (ICSE)*. IEEE, 1814–1826.

[26] Carl Hildebrandt, Meriel von Stein, and Sebastian Elbaum. 2023. PhysCov: Physical Test Coverage for Autonomous Vehicles. In *Proceedings of the 32nd ACM SIGSOFT International Symposium on Software Testing and Analysis*. 449–461.

[27] Yihan Hu, Jiazhi Yang, Li Chen, Keyu Li, Chonghao Sima, Xizhou Zhu, Siqi Chai, Senyao Du, Tianwei Lin, Wenhai Wang, Lewei Lu, Xiaosong Jia, Qiang Liu, Jifeng Dai, Yu Qiao, and Hongyang Li. 2023. Planning-oriented Autonomous Driving. In *Proceedings of the IEEE/CVF Conference on Computer Vision and Pattern Recognition*.

[28] Yuqi Huai, Sumaya Almanee, Yuntianyi Chen, Xiafa Wu, Qi Alfred Chen, and Joshua Garcia. 2023. sceno RITA: Generating Diverse, Fully-Mutable, Test Scenarios for Autonomous Vehicle Planning. *IEEE Transactions on Software Engineering* (2023).

[29] Yuqi Huai, Yuntianyi Chen, Sumaya Almanee, Tuan Ngo, Xiang Liao, Ziwen Wan, Qi Alfred Chen, and Joshua Garcia. 2023. Doppelgänger test generation for revealing bugs in autonomous driving software. In *2023 IEEE/ACM 45th International Conference on Software Engineering (ICSE)*. IEEE, 2591–2603.

[30] Yangjie Ji, Zewei Zhou, Ziru Yang, Yanjun Huang, Yuanjian Zhang, Wanting Zhang, Lu Xiong, and Zhuoping Yu. 2024. Toward autonomous vehicles: A survey on cooperative vehicle-infrastructure system. *iScience* 27, 5 (2024), 109751. doi:10.1016/j.isci.2024.109751

[31] Shinpei Kato, Shota Tokunaga, Yuya Maruyama, Seiya Maeda, Manato Hirabayashi, Yuki Kitsukawa, Abraham Monrroy, Tomohito Ando, Yusuke Fujii, and Takuya Azumi. 2018. Autoware on board: Enabling autonomous vehicles with embedded systems. In *2018 ACM/IEEE 9th International Conference on Cyber-Physical Systems (ICCPS)*. IEEE, 287–296.

[32] Seulbae Kim, Major Liu, Junghwan" John" Rhee, Yuseok Jeon, Yonghwi Kwon, and Chung Hwan Kim. 2022. DriveFuzz: Discovering Autonomous Driving Bugs through Driving Quality-Guided Fuzzing. In *Proceedings of the 2022 ACM SIGSAC Conference on Computer and Communications Security*. ACM, Los Angeles, CA, USA, 1753–1767.

[33] Hsu kuang Chiu, Ryo Hachiuma, Chien-Yi Wang, Stephen F. Smith, Yu-Chiang Frank Wang, and Min-Hung Chen. 2025. V2V-LLM: Vehicle-to-Vehicle Cooperative Autonomous Driving with Multi-Modal Large Language Models. arXiv:2502.09980 [cs.CV] https://arxiv.org/abs/2502.09980

[34] Selvaraj Vasantha Kumar. 2017. Traffic flow prediction using Kalman filtering technique. *Procedia Engineering* 187 (2017), 582–587.

[35] Guanpeng Li, Yiran Li, Saurabh Jha, Timothy Tsai, Michael Sullivan, Siva Kumar Sastry Hari, Zbigniew Kalbarczyk, and Ravishankar Iyer. 2020. AV-FUZZER: Finding safety violations in autonomous driving systems. In *2020 IEEE 31st International Symposium on Software Reliability Engineering (ISSRE)*. IEEE, Coimbra, Portugal, 25–36.

[36] Zhongrui Li, Jiarun Dai, Zongan Huang, Nianhao You, Yuan Zhang, and Min Yang. 2024. Viohawk: Detecting traffic violations of autonomous driving systems through criticality-guided simulation testing. In *Proceedings of the 33rd ACM SIGSOFT International Symposium on Software Testing and Analysis*. 844–855.

[37] Guannan Lou, Yao Deng, Xi Zheng, Mengshi Zhang, and Tianyi Zhang. 2022. Testing of autonomous driving systems: where are we and where should we go?. In *Proceedings of the 30th ACM Joint European Software Engineering Conference and Symposium on the Foundations of Software Engineering*. 31–43.

[38] Chengjie Lu, Yize Shi, Huihui Zhang, Man Zhang, Tiexin Wang, Tao Yue, and Shaukat Ali. 2022. Learning configurations of operating environment of autonomous vehicles to maximize their collisions. *IEEE Transactions on Software Engineering* 49, 1 (2022), 384–402.

[39] You Lu, Yifan Tian, Yuyang Bi, Bihuan Chen, and Xin Peng. 2024. DiaVio: LLM-Empowered Diagnosis of Safety Violations in ADS Simulation Testing. In *Proceedings of the 33rd ACM SIGSOFT International Symposium on Software Testing and Analysis* (Vienna, Austria) *(ISSTA 2024)*. Association for Computing Machinery, New York, NY, USA, 376–388. doi:10.1145/3650212.3652135

[40] Wassim G Najm, John D Smith, Mikio Yanagisawa, A John, et al. 2007. *Pre-crash scenario typology for crash avoidance research*. Technical Report. United States. Department of Transportation. National Highway Traffic Safety ....

[41] Wassim G Najm, Samuel Toma, John Brewer, et al. 2013. *Depiction of priority light-vehicle pre-crash scenarios for safety applications based on vehicle-to-vehicle communications*. Technical Report DOT HS 811 732. National Highway Traffic Safety Administration, U.S. Department of Transportation, Washington, DC.

[42] Hieu Ngo, Hua Fang, and Honggang Wang. 2023. Cooperative Perception With V2V Communication for Autonomous Vehicles. *IEEE Transactions on Vehicular Technology* 72, 9 (2023), 11122–11131. doi:10.1109/TVT.2023.3264020

[43] Philippe Nitsche, Pete Thomas, Rainer Stuetz, and Ruth Welsh. 2017. Pre-crash scenarios at road junctions: A clustering method for car crash data. *Accident Analysis & Prevention* 107 (2017), 137–151.

[44] Jan-Pieter Paardekooper, S Montfort, Jeroen Manders, Jorrit Goos, E de Gelder, O Camp, O Bracquemond, and Gildas Thiolon. 2019. Automatic identification of critical scenarios in a public dataset of 6000 km of public-road driving. In *26th International Technical Conference on the Enhanced Safety of Vehicles (ESV)*. Mira Smart, Eindhoven, Netherlands.

[45] Qi Pang, Yuanyuan Yuan, and Shuai Wang. 2022. MDPFuzz: Testing Models Solving Markov Decision Processes. In *Proceedings of the 31st ACM SIGSOFT International Symposium on Software Testing and Analysis* (Virtual, South Korea) *(ISSTA 2022)*. Association for Computing Machinery, New York, NY, USA, 378–390. doi:10.1145/3533767.3534388

[46] Federico Pratissoli, Riccardo Brugioni, Nicola Battilani, and Lorenzo Sabattini. 2023. Hierarchical traffic management of multi-AGV systems with deadlock prevention applied to industrial environments. *IEEE Transactions on Automation Science and Engineering* (2023).

[47] HongSheng Qi, Yi Yu, Qing Tang, and XianBiao Hu. 2022. Intersection traffic deadlock formation and its probability: A petri net-based modeling approach. *IET Intelligent Transport Systems* 16, 10 (2022), 1342–1363.

[48] Katrin Renz, Kashyap Chitta, Otniel-Bogdan Mercea, A. Sophia Koepke, Zeynep Akata, and Andreas Geiger. 2022. PlanT: Explainable Planning Transformers via Object-Level Representations. In *Conference on Robotic Learning (CoRL)*.

[49] Christian Roesener, Felix Fahrenkrog, Axel Uhlig, and Lutz Eckstein. 2016. A scenario-based assessment approach for automated driving by using time series classification of human-driving behaviour. In *2016 IEEE 19th international conference on intelligent transportation systems (ITSC)*. IEEE, Rio de Janeiro, Brazil, 1360–1365.

[50] Hao Shao, Letian Wang, Ruobing Chen, Hongsheng Li, and Yu Liu. 2023. Safety-enhanced autonomous driving using interpretable sensor fusion transformer. In *Conference on Robot Learning*. PMLR, 726–737.

[51] Daniel Eduardo Soltero, Stephen L. Smith, and Daniela L. Rus. 2011. Collision avoidance for persistent monitoring in multi-robot systems with intersecting trajectories. In *2011 IEEE/RSJ International Conference on Intelligent Robots and Systems*.

[52] Yang Sun, Christopher M Poskitt, Jun Sun, Yuqi Chen, and Zijiang Yang. 2022. LawBreaker: An approach for specifying traffic laws and fuzzing autonomous vehicles. In *Proceedings of the 37th IEEE/ACM International Conference on Automated*

*Software Engineering*. 1–12.

[53] Shuncheng Tang, Zhenya Zhang, Jixiang Zhou, Lei Lei, Yuan Zhou, and Yinxing Xue. 2024. Legend: A top-down approach to scenario generation of autonomous driving systems assisted by large language models. In *Proceedings of the 39th IEEE/ACM International Conference on Automated Software Engineering*. 1497–1508.

[54] Shuncheng Tang, Zhenya Zhang, Jixiang Zhou, Yuan Zhou, Yan-Fu Li, and Yinxing Xue. 2023. EvoScenario: Integrating Road Structures into Critical Scenario Generation for Autonomous Driving System Testing. In *2023 IEEE 34th International Symposium on Software Reliability Engineering (ISSRE)*. 309–320. doi:10.1109/ISSRE59848.2023.00054

[55] Wenbing Tang, Mingfei Cheng, Yuan Zhou, and Yang Liu. 2025. Moral Testing of Autonomous Driving Systems. *arXiv preprint arXiv:2505.03683* (2025).

[56] Yun Tang, Yuan Zhou, Yang Liu, Jun Sun, and Gang Wang. 2021. Collision avoidance testing for autonomous driving systems on complete maps. In *2021 IEEE Intelligent Vehicles Symposium (IV)*. IEEE, Nagoya, Japan, 179–185.

[57] Yun Tang, Yuan Zhou, Fenghua Wu, Yang Liu, Jun Sun, Wuling Huang, and Gang Wang. 2021. Route coverage testing for autonomous vehicles via map modeling. In *2021 IEEE International Conference on Robotics and Automation (ICRA)*. IEEE, Xi'an, China, 11450–11456.

[58] Yun Tang, Yuan Zhou, Tianwei Zhang, Fenghua Wu, Yang Liu, and Gang Wang. 2021. Systematic testing of autonomous driving systems using map topology-based scenario classification. In *Proceedings of the 36th IEEE/ACM International Conference on Automated Software Engineering (ASE)*. IEEE, Melbourne, Australia, 1342–1346.

[59] Gokulnath Thandavarayan, Miguel Sepulcre, and Javier Gozalvez. 2020. Cooperative Perception for Connected and Automated Vehicles: Evaluation and Impact of Congestion Control. *IEEE Access* 8 (2020), 197665–197683. doi:10.1109/ACCESS.2020.3035119

[60] Eric Thorn, Shawn C Kimmel, Michelle Chaka, Booz Allen Hamilton, et al. 2018. *A framework for automated driving system testable cases and scenarios*. Technical Report. United States. Department of Transportation. National Highway Traffic Safety.

[61] Sebastian Thrun. 2002. Probabilistic robotics. *Commun. ACM* 45, 3 (2002), 52–57.

[62] Haoxiang Tian, Yan Jiang, Guoquan Wu, Jiren Yan, Jun Wei, Wei Chen, Shuo Li, and Dan Ye. 2022. MOSAT: finding safety violations of autonomous driving systems using multi-objective genetic algorithm. In *Proceedings of the 30th ACM Joint European Software Engineering Conference and Symposium on the Foundations of Software Engineering*. 94–106.

[63] Robin van der Made, Martijn Tideman, Ulrich Lages, Roman Katz, and Martin Spencer. 2015. Automated generation of virtual driving scenarios from test drive data. In *24th International Technical Conference on the Enhanced Safety of Vehicles (ESV) National Highway Traffic Safety Administration*.

[64] Renzhi Wang, Mingfei Cheng, Xiaofei Xie, Yuan Zhou, and Lei Ma. 2025. MoDitector: Module-Directed Testing for Autonomous Driving Systems. *arXiv preprint arXiv:2502.08504* (2025).

[65] Tsun-Hsuan Wang, Sivabalan Manivasagam, Ming Liang, Bin Yang, Wenyuan Zeng, and Raquel Urtasun. 2020. V2VNet: Vehicle-to-Vehicle Communication for Joint Perception and Prediction. In *Computer Vision – ECCV 2020*, Andrea Vedaldi, Horst Bischof, Thomas Brox, and Jan-Michael Frahm (Eds.). Springer International Publishing, Cham, 605–621.

[66] Waymo. 2024. Waymo One Autonomous Ride-Hailing in San Francisco. https://waymo.com/intl/zh-cn/waymo-one-san-francisco/ Accessed: 2025-05-16.

[67] Greg Welch, Gary Bishop, et al. 1995. An introduction to the Kalman filter. (1995).

[68] Runsheng Xu, Yi Guo, Xu Han, Xin Xia, Hao Xiang, and Jiaqi Ma. 2021. OpenCDA: an open cooperative driving automation framework integrated with co-simulation. In *2021 IEEE International Intelligent Transportation Systems Conference (ITSC)*. IEEE, 1155–1162.

[69] Zhongxia Yan, Abdul Rahman Kreidieh, Eugene Vinitsky, Alexandre M. Bayen, and Cathy Wu. 2023. Unified Automatic Control of Vehicular Systems With Reinforcement Learning. *IEEE Transactions on Automation Science and Engineering* 20, 2 (2023), 789–804. doi:10.1109/TASE.2022.3168621

[70] Zhongxia Yan, Han Zheng, and Cathy Wu. 2024. Multi-agent path finding for cooperative autonomous driving. In *2024 IEEE International Conference on Robotics and Automation (ICRA)*. IEEE, 12361–12367.

[71] Xudong Zhang and Yan Cai. 2023. Building Critical Testing Scenarios for Autonomous Driving from Real Accidents. In *Proceedings of the 32nd ACM SIGSOFT International Symposium on Software Testing and Analysis*. 462–474.

[72] Xiaodong Zhang, Wei Zhao, Yang Sun, Jun Sun, Yulong Shen, Xuewen Dong, and Zijiang Yang. 2023. Testing automated driving systems by breaking many laws efficiently. In *Proceedings of the 32nd ACM SIGSOFT International Symposium on Software Testing and Analysis*. 942–953.

[73] Zhejun Zhang, Alexander Liniger, Dengxin Dai, Fisher Yu, and Luc Van Gool. 2021. End-to-end urban driving by imitating a reinforcement learning coach. In *Proceedings of the IEEE/CVF international conference on computer vision*. 15222–15232.

[74] Ziyuan Zhong, Gail Kaiser, and Baishakhi Ray. 2023. Neural network guided evolutionary fuzzing for finding traffic violations of autonomous vehicles. *IEEE Transactions on Software Engineering* 49, 4 (2023), 1860–1875.

[75] Yuan Zhou, Yang Sun, Yun Tang, Yuqi Chen, Jun Sun, Christopher M Poskitt, Yang Liu, and Zijiang Yang. 2023. Specification-based Autonomous Driving System Testing. *IEEE Transactions on Software Engineering* (2023), 1–19.